

Joint Offshore Wind and Wave Energy Resources in the Caribbean Sea

Brandon J. Bethel¹

Received: 27 February 2021 / Accepted: 6 May 2021 / Published online: 9 December 2021
© Harbin Engineering University and Springer-Verlag GmbH Germany, part of Springer Nature 2021

Abstract

Complementarities between wind and wave energies have many significant advantages that are unavailable with the sole deployment of either. Using all available wind speed, significant wave height, and wave period buoy observations over a 10-year period (i.e., 2009–2019), colocated wind and wave energy resources are estimated. Although buoy records are imperfect, results show that the inner Caribbean Sea (CS) under the influence of the Caribbean low-level jet has the highest wind energy resource at $\sim 1500 \text{ W/m}^2$, followed by the outer CS at $\sim 600 \text{ W/m}^2$ and Atlantic Ocean (AO) at $\sim 550\text{--}600 \text{ W/m}^2$ at a 100 m height. Wave energy was most abundant in the AO at 14 kW/m , followed by the inner CS at 13 kW/m and outer CS at 5 kW/m . The average and dominant wave energies can reach a maximum of 10 and 14 kW/m , respectively. Asymmetry between wind and wave energy resources is observed in the AO, where wave energy is higher than the low wind speed/energy would suggest. Swell is responsible for this discrepancy; thus, it must be considered not only for wave energy extraction but also for wind turbine fatigue, stability, and power extraction efficiency.

Keywords Wave energy · Wind energy · Colocation · Caribbean Sea · Small island developing states · NDBC buoys

1 Introduction

For the Caribbean Sea (CS), which is nearly completely inhabited by small island developing states (SIDS) that are intrinsically linked to the sea, ocean renewable energy provides a significant avenue toward transitioning to blue economy activities that have the potential to restart and revitalize economies shattered by the global shutdown of tourism in the COVID-19 era (Ochs et al. 2015; IRENA 2020). Offshore wind energy is a mature and economically viable

source of electricity, whereas offshore wave energy is the subject of intense research and a few commercial ventures. Alone, wave energy is a natural choice to harness for several crucial reasons: its forecast accuracy is higher (geographic dispersal increases this accuracy; Reikard et al. 2015), and grid integration costs (as measured by quantifying balancing reserves) are cheaper than either wind or solar energy. Moreover, its energy density and employment potential are higher than either wind or solar energy (Akar and Akdoğan 2016). However, the compatibility of wind and wave energies is demonstrated in the colocation of wind and wave generators to achieve several benefits that include but are not limited to reducing power output variability (Gideon and Bou-Zeid 2021), energy costs, and environmental impact (Astariz et al. 2015a; Azzellino et al. 2019), increasing accessibility to wind turbines and operations and maintenance (O&M) activities, sharing electrical infrastructure (Astariz and Iglesias 2015; Astariz et al. 2015b, 2015c), ensuring efficiency and reliability (Gao et al. 2021), and quickening the pace of wave energy development to be on par with wind energy (Astariz and Iglesias 2015). Research into technologies to integrate wind and wave farms is rapidly advancing (Homayoun et al. 2019; Mazarakos et al. 2019; Pérez-Collazo et al. 2019; Gkaraklova et al. 2020; Wang et al. 2020), with numerous methodologies available to estimate the feasibility

Article Highlights

- Wind and wave energy are jointly estimated in the Caribbean Sea and the Atlantic Ocean from 2009 to 2019.
- Wind and wave energy, respectively, were measured at $\sim 1500 \text{ W/m}^2$ and 13 kW/m in the inner Caribbean Sea under the direct influence of the Caribbean low-level jet.
- Dominant wave energy was most abundant in the Atlantic Ocean and was measured at 14 kW/m .
- There is an asymmetry between wind and wave energy resources in the Atlantic Ocean, and this is primarily thought to be due to the influence of swell.

✉ Brandon J. Bethel
20195109101@nuist.edu.cn

¹ School of Marine Sciences, Nanjing University of Information Science & Technology, Nanjing 210044, China

of these colocated farms. For example, Astariz and Iglesias (2017) proposed an index for colocated wind and wave farms based on the variability and correlation between waves and winds, in addition to user conflicts, environmental conservation, and economic development. In a similar vein, Louko-georgaki et al. (2018) provided a framework for evaluating marine areas suitable for wind and wave energy systems by incorporating a variety of environmental, economic, technical, and sociopolitical aspects.

Islands, particularly SIDS, are ideal locations for the development of renewable energy (Klöck 2016; Kuang et al. 2016; Bundhoo 2017; Chen et al. 2020; Koon et al. 2020; Sterl et al. 2020; Praene et al. 2021). Although neither is a baseload power source, winds and waves are attractive energy sources, leading Rusu and Onea (2019) to investigate the wind and wave potentials in islands across the globe, inclusive of the CS nation of Cuba. However, the literature only documents energy assessments of either winds or waves, rather than both simultaneously. Because of scarce instrumentation in the CS, Ortega et al. (2013) used a numerical wave model to identify optimum wave farm sites. Appendini et al. (2015) performed a 30-year hindcast of waves in the CS and determined that the Caribbean low-level jet (CLLJ), which is an easterly zonal wind reaching 13 m/s, governed the region's wave climatology, producing 8–14 kW/m of wave energy. Although semi-enclosed, the windward sides of the Lucayan Archipelago and the Greater and Lesser Antilles coastlines are affected by waves from the AO and thus may have a large part of their wave energy delivered by swell rather than wind sea (de Farias et al. 2012; Jury 2018; Zheng et al. 2016; Christakos et al., 2020a, b). Indeed, Garcia and Canals (2015), Jury (2018), and Silander and Moreno (2019) have shown through buoy observations and numerical models that swell accounts for a large proportion of wave energy on northern Puerto Rico and US Virgin Island coastlines. Guillou et al. (2020), using wave hindcast, determined that, in addition to the CLLJ increasing wave power in the CS, the Lesser Antilles is an attractive area to harvest wave energy because of more regular wave conditions. Chadee and Clarke (2014) assessed wind energy using reanalysis data and estimated that the area means reached a maximum of 592 W/m². Rueda-Bayona et al. (2019) used satellite data to revise an earlier assessment and estimated that, in the Colombian regions of La Guajira, Barranquilla, and Santa Marta, the area means ranged from 482 to 658 W/m² at various atmospheric heights. Arce and Bayne (2020) analyzed offshore wind energy in Colombia and discussed in detail the challenges and opportunities of the industry, in conjunction with the technical and economic perspectives. Chadee et al. (2017) used the Weather Research and Forecasting numerical atmospheric model to map near-surface wind energy resources in Trinidad and Tobago. In a subsequent economic assessment, Chadee and Clarke (2018)

determined that large wind turbines would be cost-competitive for Caribbean SIDS.

To the best of the author's knowledge, no studies have considered the simultaneous evaluation of colocated wind and wave energy resources in the Caribbean. Because of the synergy between the maturity of wind energy exploitation and the increasing projections of wind energy availability (Costoya et al. 2019), the suggestion that, although the region has one of the world's lowest wave energy potentials, it could still be a practical area for wave energy harvesting (Lemessy et al. 2019), and the need to accelerate the development of regional renewable energy utilization to achieve Goal 7 of the United Nations Sustainable Development Goals, the remainder of this paper is structured as follows: Section 2 describes the data and methodology. Section 3 presents the results. Sections 4 and 5, respectively, provide a discussion and conclusion.

2 Data and Methodology

2.1 Observational Data and Measurement Description

Six buoys deployed throughout the CS (Figure 1) and maintained by the National Buoy Data Center (NDBC) are accessed for their observations of surface wind speed, wind direction, significant wave height, average and dominant

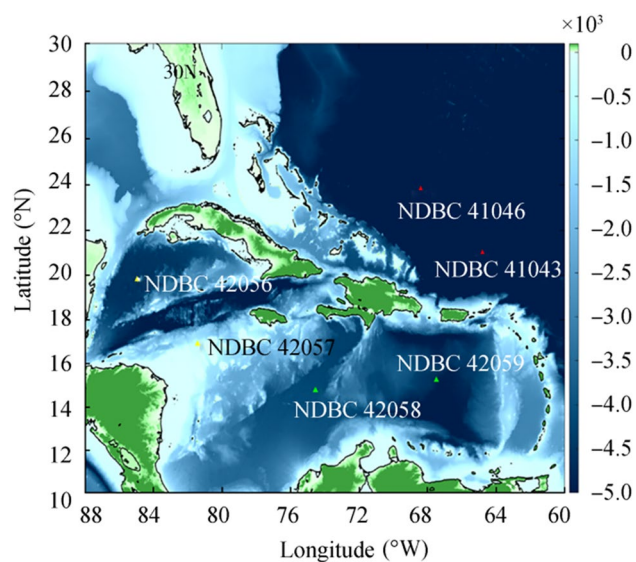


Figure 1 Shading is the bathymetry and topography (units: m) of the Caribbean Sea with NDBC buoy locations marked. The green, yellow, and red triangles denote the inner CS, outer CS, and Atlantic Ocean buoys, respectively

wave periods, and mean wave direction (Table 1) to perform the analyses. Surface wind speed (m/s) is the wind speed averaged over an 8-min period and is reported every 10 min or hourly. Where applicable, 10-min wind speed is resampled to ensure a uniform hourly resolution. Wind direction (i.e., the direction that the wind is coming from in degrees clockwise from true north) is measured during the same period as wind speed. Significant wave height (m) is calculated as the average of the highest one-third of all wave heights during a 20-min sampling period. Dominant wave period (s) is the period with the maximum wave energy (either wind sea or swell), and average wave period (s) is the average of all waves during a 20-min period. Mean wave direction is the direction from which waves at the dominant period are coming. It is measured in degrees from true north and increases clockwise with north as 0° and east as 90° . For additional information on measurement descriptions and units, the readers are directed to <https://www.ndbc.noaa.gov/wave.shtml>. Although the NDBC performs spectral partitioning of its wave data into separate wind wave and swell wave properties and is of interest in this study, only real-time data, which do not exist in historical files, are provided. An alternative for the discrimination of wave systems is provided in Sect. 2.2.3. Wind speed is converted from its anemometer height into its 10 and 100 m heights through the logarithmic law:

$$u_{10100} = u_h \frac{\ln\left(\frac{h}{z_0}\right)}{\ln\left(\frac{z_{\text{ref}}}{z_0}\right)} \quad (1)$$

where u_h and u_{10100} (m/s) are the wind speed at the buoy anemometer height (Table 1), h is the reference height, and z_0 is the roughness length equal to 0.01, which corresponds to normal sea conditions. Although the roughness length under open sea conditions is smaller (i.e., 0.0002), the studies conducted by Frank et al. (2000) and Barthelmie (2001) both show that, when wind speed is extrapolated to heights greater than 10 m above sea level, variability in the sea surface roughness length is too small to have a noticeable

impact on wind resources at typical hub heights (Barthelmie et al. 2007). As this value is widely used in other studies (e.g., Ma et al. 2021), it will also be used here to ensure consistency.

2.2 Methodology

2.2.1 Wind Power Estimation

Given a sufficiently long time series of wind speed data for a given region, the wind power density P per unit area A can be calculated as follows:

$$\frac{P}{A} = \frac{1}{2} \rho v^3 \quad (2)$$

where v is the wind speed (m/s) and ρ is the air density (1.025 kg/m^3).

2.2.2 Wave Power Estimation

In deep water, where the wavelength is smaller than twice the water depth, wave power may be directly calculated from the wave height (H_s) and average (T_{apd}) or dominant (T_{dpd}) wave energy period, as follows:

$$P = \frac{\rho g^2}{64\pi} H_s^2 T_{\text{apd,dpd}} \quad (3)$$

where ρ is the seawater density (1025 kg/m^3), $T_{\text{apd,dpd}}$ is the average (apd) or dominant (dpd) energy period, and g is the gravitational acceleration (9.8 m/s^2). Noting that the standard wave energy equation may cause significant errors in shallow water ($h < L/2$; Ozkan and Mayo 2019), the shallow water condition was not met for all buoys.

2.2.3 Quasi-wave Age

Because the NDBC does not archive spectrally partitioned wave information, discrimination between wind sea and

Table 1 National Buoy Data Center buoy statistics

NDBC ID	Latitude ($^\circ\text{N}$)	Longitude ($^\circ\text{W}$)	Anemometer height (m)	Water depth (m)	No. of wind observations	Wind data availability (%)	No. of wave observations	Wave data availability (%)
41043	21.030	64.790	3.8	5262	92937	96.4	94569	98.1
41046	23.822	68.384	3.8	5549	93968	97.5	93024	96.5
42056	19.820	84.945	4.1	4554	76114	78.9	84581	87.8
42057	16.906	81.422	3.8	377	75434	78.2	78189	81.1
42058	14.776	74.548	3.8	4158	73286	76	71328	73.9
42059	15.252	67.483	4.1	4784	73442	76.2	65337	67.8

swell is achieved by computing the quasi-wave age (Glazman and Pilorz 1990) for each buoy, as follows:

$$\beta' = 3.24 \times \left(\frac{gh}{u^2} \right)^{0.62} \quad (4)$$

where β' is the quasi-wave age, g is the gravitational acceleration, h is the significant wave height, and u is the wind speed at 10 m. Waves are categorized as swell when $\beta' > 4$; otherwise, they are categorized as wind waves.

3 Results

3.1 Wind Energy Estimates

Given its commercial and technological maturity, the annual average wind power is plotted in Figure 2. In comparison with all other stations, NDBC buoy 42058 has the highest average wind power by far, peaking at $\sim 1800 \text{ W/m}^2$ in 2015, primarily because it is situated near the main 15° N axis of the CLLJ and in the inner CS. NDBC buoy 42059 has the second-highest average wind power, peaking at approximately 1000 W/m^2 in 2018. The outer CS buoys (i.e., 42056 and 42057) have roughly the same level of wind energy as the AO buoys (i.e., 41043 and 41046), fluctuating between 600 and 800 W/m^2 . Excluding buoy 42057, all other buoys are located and installed in deep water ($\geq 4000 \text{ m}$; Figure 1), which would require floating offshore wind turbines to be installed; although this is a more expensive option, it is preferable because of visual and noise pollution, in addition to impacts on wildlife that characterize land-based and nearshore wind turbines (Wolsink 2010; Jensen et al. 2014; Lee et al. 2020; Dugstad et al., 2020). Moreover, although the wind power of buoys 41043, 41046, 42056, and 42057 are lower than that of buoys 42058 and 42059

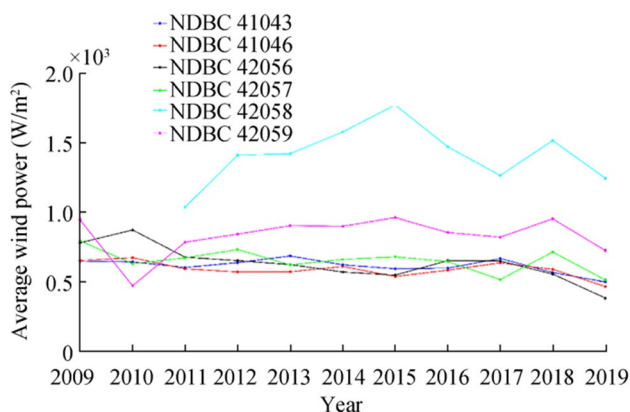


Figure 2 Annual average wind power (W/m^2) at the six NDBC buoy locations

that lie directly under the CLLJ, its annual fluctuations are less severe. Although wind energy resources are primary considerations for extraction, atmospheric stability is of greater significance for long-term project viability (Ramos et al. 2017; Corrêa Radünz et al. 2020; Pryor et al. 2020).

3.2 Wave Energy Estimates

Colocated annual estimates of average and dominant wave energies for each buoy are shown in Figure 3. As expected, when the dominant wave period is used to calculate wave energy, its value in each case is a minimum of $\sim 2 \text{ kW/m}$ higher than the average wave energy. Wave energy converters (WECs) that are tuned to the dominant wave period, rather than the average wave period, have two main benefits. Primarily, for wave climates with low wave energy potential, selecting locations with even moderately higher values of energy increases the commercial viability of such projects as tuning the natural frequency of a WEC to incoming waves enables resonant mode operation and amplifies its velocity, which is quadratically proportional to the extracted energy (Maria-Arenas et al. 2019). Secondly, WEC power absorption bandwidths are maximized during optimization processes when devices are tuned to the predominant wave period of a given site (Shadman et al. 2018). In the AO, for buoys 41,043 and 41,046, dominant wave energy can reach values greater than 12 kW/m and decrease to approximately 8 kW/m when the average is considered.

This result is incongruent with prior estimates of wind energy and will be discussed in the subsequent section. Notably, the annual fluctuations at buoy 41,046 are less severe than further south at buoy 41043 with similar levels of wave energy, indicating that wave energy there would be more stable. However, for buoys 42056 and 42057 in the outer CS, dominant wave energy is less abundant, reaching approximately 6 kW/m before decreasing to $\geq 4 \text{ kW/m}$ over the 10-year period. Under the direct influence of the CLLJ, this trend is reversed for buoy 42058 where dominant wave energy exceeds 16 kW/m and the average peaks at approximately 12 kW/m . Although the resources here are abundant, it is influenced by the waxing and waning of the CLLJ (Appendini et al. 2015) and thus is not as stable as the resources in the outer CS. At some distance from buoy 42058, buoy 42059 has higher dominant and average wave energy values and higher annual stability than either buoy 42056 or 42057.

In Figure 4, when wind and wave energies for each buoy location are compared, it is largely true that where wind energy is high (buoys 42,058 and 42059), wave energy is also high, which is expected because of the close relationship between wind speed and wave growth. However, another more interesting pattern emerges. Based on the observations that the wind energies for buoys 41043 and 41046 at approximately 500 W/m^2 are low and the two

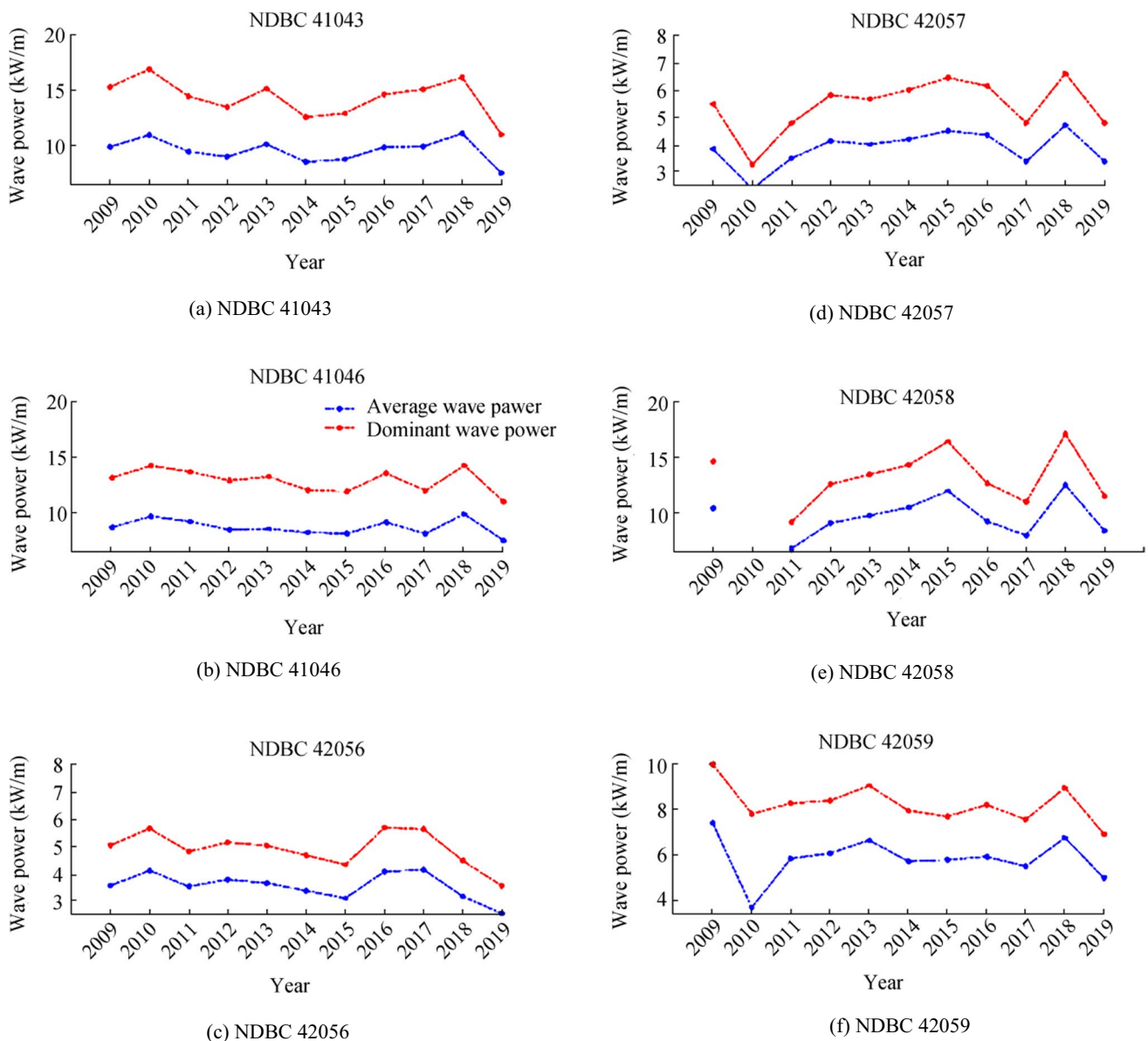


Figure 3 Annual average (blue) and dominant (red) wave power (kW/m) at the six NDBC buoy locations

lowest among the six buoys (Figure 4a), they nevertheless have similar wave energies to buoy 42,058 that has the highest wind energy at $\sim 1500 \text{ W/m}^2$. This is true for either average wave energy (Figure 4b) or dominant wave energy (Figure 4c). Given that wind energy is directly proportional to the cube of the wind speed, the wave energy shown in either Figure 4b or c could not be due solely to the input of energy from the wind. If wind input did not translate directly into wave growth, then another energy source is required to explain the discrepancy between wind and wave energies. As both buoys 41043 and 41046 lie within the AO, swell could contribute to total wave energy, which will be discussed in the subsequent section.

3.3 Quasi-wave Age and Wind/Wave (Mis)alignment

To confirm the hypothesis that the large discrepancy between wind and wave energies in the AO was due to swell, two representative buoys for the AO (NDBC buoy 41043) and CS (NDBC buoy 42059) were selected and the quasi-wave age (Eq. (4)) for 2019 was calculated. As is already well understood, wind sea is generated directly by wind input and thus is highly correlated and sensitive to the wind speed and direction among other variables, which leads to a host of studies of the optimum wind forcing configurations for numerical wave models (Wang et al. 2018; Christakos et al., 2020a, b; Optis et al. 2021; Liu et al. 2021) and investigations into how

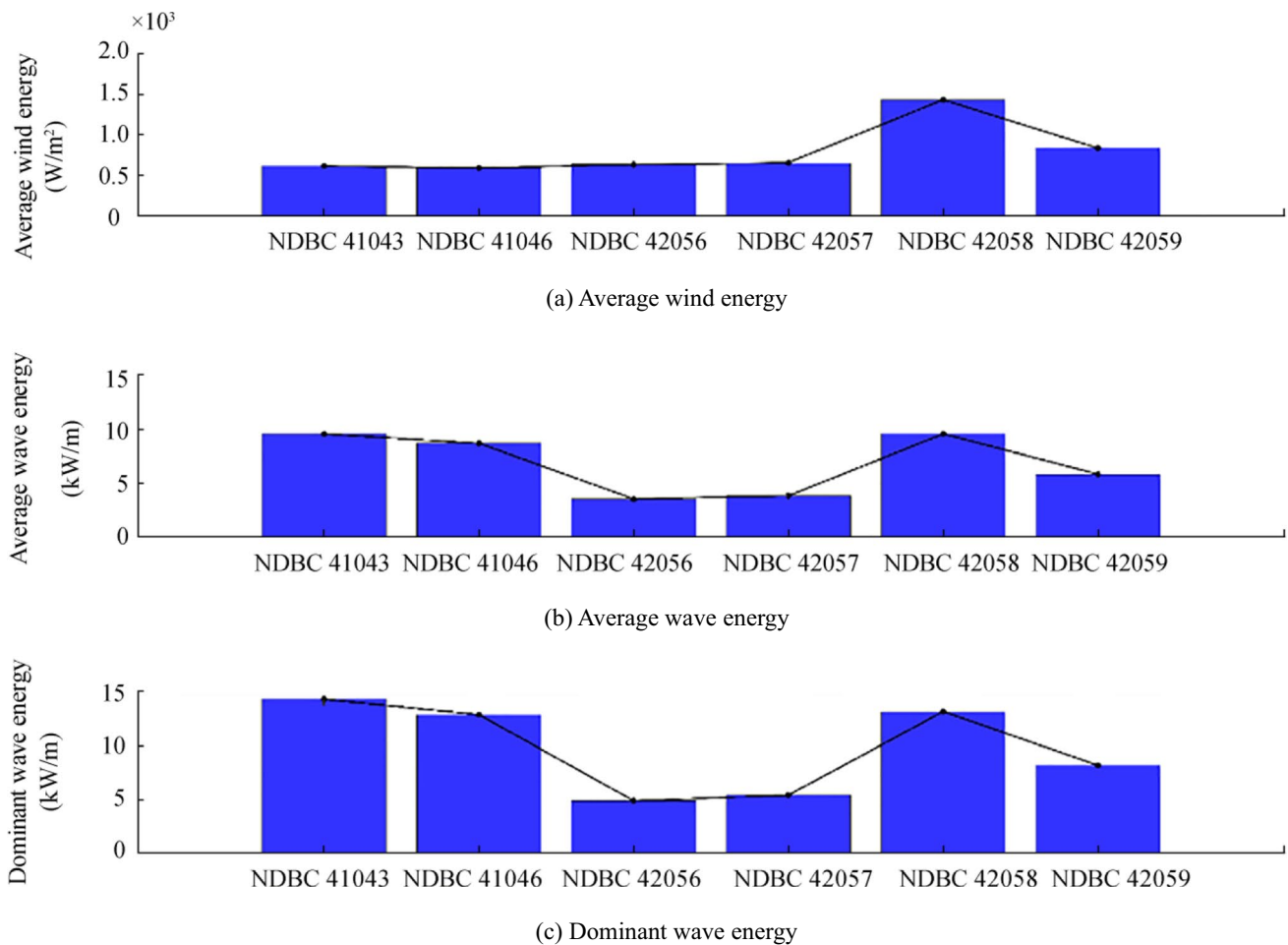


Figure 4 Comparison of average wind, average wave, and dominant wave energies for each buoy over a 10-year period (i.e., 2009–2019)

long-term changes in either variable may affect coastal communities, offshore operations, and shipping routes (Rusu et al. 2018). By contrast, swell is inert to the overlying wind field, can propagate across ocean basins with minor attenuation, and has been shown to dominate the north AO, particularly in the summer (Semedo et al. 2008, 2011). Figure 5 shows a histogram of the quasi-wave age for either buoy, with the wind sea/swell determinant (wave age = 4) plotted. Waves with ages larger than 35, which are ignored here but do exist in the record, are due to storm/hurricane activity. The frequency occurrence is measured from 0 to 1. Notably, the CS (blue) is overwhelmingly governed by extremely young waves (0–2), i.e., wind sea, that occur nearly all of the time. For less than 10% of the time, older waves (~ 3 –4) also occur, with any even older waves occurring for less time. This is strongly contrasted by waves in the AO at buoy 41043 (red), where older waves (4–6), thus indicating swell, occur for a little over 50% of the time. Although their occurrence is significantly less frequent than this, even older waves (≥ 5) exist. A significantly stronger correlation between wind speed and wave height is observed

for NDBC buoy 42059 ($\text{CORR} = 0.67$) than for NDBC buoy 41043 ($\text{CORR} = 0.37$), which enables the discrimination between wind sea and swell.

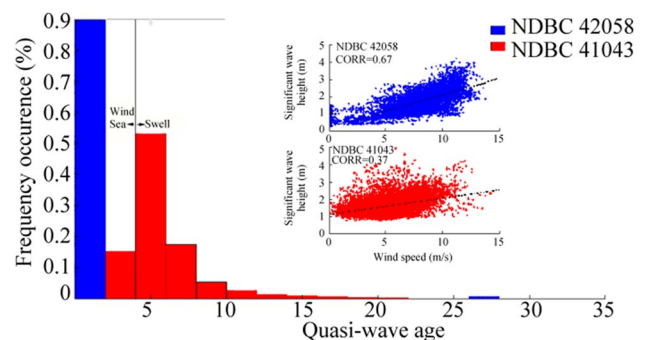


Figure 5 Histograms of quasi-wave age for NDBC buoys 42058 and 41043 (blue and red, respectively); in the insets, scatter plots of significant wave height and wind speed are given (NDBC buoy 42058, blue; NDBC buoy 41043, red)

As swell is relatively insensitive to wind speed, it is also often misaligned with wind direction. Crucially, offshore platforms and wind turbines installed in seas where there is misalignment between winds and waves cause increases in fatigue damage, construction time, and costs (Hildebrandt and Cossu 2018; Hildebrandt et al. 2019; Kang and Yang 2019; Porchetta et al. 2019; Sørsum et al. 2019; Verma et al. 2020; Wei et al. 2021). In Figure 6, the difference between wave and wind directions ($\Delta\theta$) was calculated for NDBC buoys 42058 and 41043 for the year 2019. For buoy 42058 (blue) installed in the CS under direct CLLJ forcing with $\Delta\theta$ that can reach up to $\sim 60^\circ$, the bulk of measurements lies between approximately 30 and 60° . By contrast, for buoy 41043 (red), although the wind and wave directions were nearly frequently aligned ($< \pm 30^\circ$), $\Delta\theta$ for buoy 41043 extended beyond the maximum of buoy 42058 to over $\pm 180^\circ$. These results indicate that, although a large proportion of wind sea was observed at buoy 41,043 in the AO, swell that was misaligned with the local wind was also observed. Thus, if offshore wind platforms are placed in the AO in a colocated configuration with WECs, then the effects of the large deviation between wind and wave directions must be considered. Although swell accounts for a large proportion of wave energy in the AO and offsets the disadvantage from overlying lower wind speeds compared with that in the CS, Al Sam et al. (2017) demonstrated that swell moving faster than the wind and aligned with the local wind direction may increase wind turbine power extraction rates, thus providing an additional benefit. However, this must be tempered by the effects that swell would have on the motion of a floating structure.

4 Discussions

Wind energy resources in the CS have a similar magnitude to those in other high-potential, low-latitude sites, such as south of the Hawaiian Islands, the Somalian coast, and

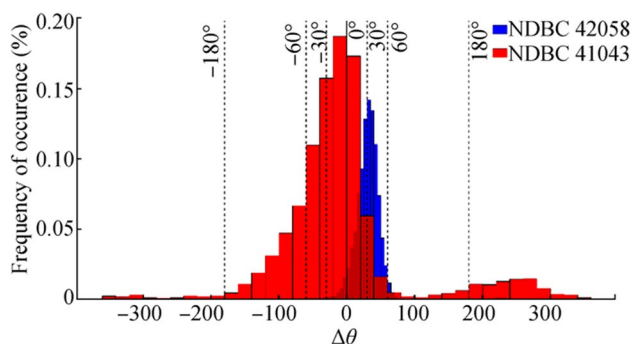


Figure 6 Histograms of the difference between wind and wave directions ($\Delta\theta$) for NDBC buoys 42058 (blue) and 41043 (red) for the year 2019

the Peruvian western offshore, because of the presence of coastal low-level jets. This results in an International Electrotechnical Commission (IEC) Class I classification as the annual average wind speed in these areas meet and exceed 10 m/s. However, in the northern CS and AO, the annual average wind speed decreases to approximately 6.5 m/s, resulting in an IEC Class III classification and thus necessitating the use of different types of turbines throughout the region. Wave energy resources in semi-enclosed seas, such as the Mediterranean, Red, Black, and Baltic Seas, are low (e.g., ≥ 4.5 kW/m in the Red Sea) because of minimal fetches for wave growth and/or the absence of low-level jets. However, the results indicate that wave energy is significantly higher in the CS and AO. Thus, compared with other sites with low (≤ 20 kW/m) wave energy potential sites, the CS and AO have many times the energy potential and thus are attractive areas to harvest wave energy. As a site with less hostile offshore wave conditions compared with highly energetic locations, the region can utilize WECs that are not as robustly designed and thus should be cheaper while converting commercially adequate volumes of wave energy into electricity. By harnessing wind and wave renewable energy resources, Goal 7 of the United Nations Sustainable Development Goals can be partially achieved, yet exploitation must be balanced against regional realities. Caribbean nations rely primarily on their unspoiled natural environments to attract tourists to support their economies and install wind turbines/WECs nearshore to minimize electricity transmission, and O&M costs may be politically polarizing and serve as an additional factor that retards industry growth. As a result, colocated wind and wave farms should have layout algorithms to take tourism-related user conflicts into higher consideration than may be allocated for other regions. Although not discussed in this study, device survivability is also a pressing issue as hurricane activity is frequent and consequently, whether directly through intense wind speed or indirectly through hurricane-induced waves, influences platform design. Taking these and other issues into account, subsequent studies should aim at quantifying electricity production using state-of-the-art wind turbines and WECs considering resource availability, stability, survivability, and sea space user conflicts.

5 Conclusions

For an extremely mature source of renewable energy, wind energy development is, quite paradoxically, rather limited in its application throughout the CS. Wave energy development is also nearly nonexistent. For coastal communities and SIDS throughout the region, harnessing these and other forms of renewable energy provides pathways to revitalize economies overly dependent on tourism that stalled in the

wake of the COVID-19 pandemic by blue economy activities that usher in blue recovery and growth. This study conducted a preliminary resource assessment of offshore winds and waves, considering the symbiotic relationship that exists between energy extraction technologies. The results showed that wind energy was most abundant at buoy 42058 under the direct influence of the CLLJ, reaching $\sim 1500 \text{ W/m}^2$. As expected, dominant wave energy was also most abundant at this location, exceeding 16 kW/m with a mean of 13 kW/m . However, variability and distance from the coastline are issues that must be considered for either wind turbine or WEC installations. Further away but still relatively under forcing by the CLLJ, buoy 42059 had, in comparison with buoy 42058, lower wind and wave energy resources (measured at $\sim 1000 \text{ W/m}^2$ and $\leq 10 \text{ kW/m}$, respectively) but still exceeded the remaining CS locations as both buoys 42056 and 42057 lie far outside the influence of the CLLJ and are located near Cuba. In either buoy 42056 or 42057, wind and wave energies were the least abundant of any buoy and were measured at $\leq 600 \text{ W/m}^2$ and $\leq 5 \text{ kW/m}$, respectively. In the AO, an unexpected discrepancy between wind and wave energy resources was observed. Wind energies for buoys 41043 and 42046 were measured at approximately 500 W/m^2 , and the average and dominant wave energies reached approximately $10\text{--}15 \text{ kW/m}$. In the AO, wind energy had roughly the same magnitude as that observed in the outer CS (buoys 42056 and 42057) yet had double to triple the wave energy resource. This discrepancy was attributed to the existence of swell in the AO that could transport energy to the windward sides of the Lucayan Archipelago and the Greater and Lesser Antilles coastlines. Thus, two roughly discrete wave regimes characterized by wind sea inside the CS and swell on the eastern island boundaries are responsible for the differences in wave energy. This has important implications for offshore wind turbine stability and energy extraction and dictates the WEC operating parameters. To foster continued research into renewable energy resource exploitation along with other blue economy activities, Caribbean governments should follow the example of Antigua and Barbuda in establishing a Centre for Excellence for Oceanography and the Blue Economy at The University of the West Indies Five Islands Campus and make strong investments in broadening ocean literacy, ocean in situ and remote sensing observation platforms, and computational resources. At the onset of the United Nations Decade of Ocean Science for Sustainable Development (2021–2030), Caribbean governments should take advantage of financial, technical, and technological support made available by global partners to other coastal communities and SIDS across the planet.

Acknowledgements We thank the National Buoy Data Center for providing the buoy observations used in this paper.

References

- Al Sam A, Szasz R, Revstedt J (2017) Wind-wave interaction effects on a wind farm power production. *J Energy Resour Technol* 139(5):051213. <https://doi.org/10.1115/1.4036542>
- Akar S, Akdoğan DA (2016). Environmental and economic impacts of wave energy. In: M. Mustafa Erdoğan, et al. (Eds.). *Some public policy recommendations for implementation. Handbook of Research on Green Economic Development Initiatives and in Turkey*. IGI Global, 285–309. <https://doi.org/10.4018/978-1-5225-0440-5.ch013>
- Appendini CM, Urbano-Latorre CP, Figueroa B, Dagua-Paz CJ, Torres-Freyermuth A, Salles P (2015) Wave energy potential assessment in the Caribbean low level jet using wave hindcast information. *Appl Energy* 137:375–384. <https://doi.org/10.1016/j.apenergy.2014.10.038>
- Arce L, Bayne S (2020) Analysis of offshore wind energy in Colombia: current status and future opportunities. *International Journal of Engineering Research* 9(11):610–619. <https://doi.org/10.17577/IJERTV9IS110277>
- Astariz S, Perez-Collazo C, Abanades J, Iglesias G (2015a) Co-located wave-wind farms: economic assessment as a function of layout. *Renew Energy Elsevier* 83(C):837–849. <https://doi.org/10.13140/RG.2.1.3392.5285>
- Astariz S, Abanades J, Pérez-Collazo C, Iglesias G (2015b) Improving wind farm accessibility for operation & maintenance through a co-located wave farm: influence of layout and wave climate. *Energy Convers Manage* 95:229–241. <https://doi.org/10.1016/j.enconman.2015.02.040>
- Astariz S, Pérez-Collazo C, Abanades J, Iglesias G (2015c) Co-located wind-wave farm synergies (operation & maintenance): a case study. *Energy Convers Manage* 95:63–75. <https://doi.org/10.1016/j.enconman.2014.11.060>
- Astariz S, Iglesias G (2015) Enhancing wave energy competitiveness through co-located wind and wave energy farms. A review on the shadow effect. *Energies* 9:7344–7366. <https://doi.org/10.3390/en8077344>
- Astariz S, Iglesias G (2017) The collocation feasibility index – a method for selecting sites for co-located wave and wind farms. *Renewable Energy* 103:811–824. <https://doi.org/10.1016/j.renene.2016.11.014>
- Azzellino A, Lanfredi C, Riefolo L, De Santis V, Contestabile P, Vicinanza D (2019) Combined exploitation of offshore wind and wave energy in the Italian seas: a spatial planning approach. *Front Energy Res* 7:42. <https://doi.org/10.3389/fenrg.2019.00042>
- Barthelmie RJ (2001) Evaluating the impact of wind induced roughness change and tidal range on extrapolation of offshore vertical wind speed profiles. *Wind Energy* 4(3):99–105. <https://doi.org/10.1002/we.45>
- Barthelmie RJ, Badger J, Pryor SC, Hasager CB, Christiansen MB, Jørgensen BH (2007) Offshore coastal wind speed gradients: issues for the design and development of large offshore wind-farms. *Wind Eng* 31(6):369–382. <https://doi.org/10.1260/030952407784079762>
- Bundhoo ZMA (2017) Renewable energy exploitation in the small island developing state of Mauritius: current practice and future potential. *Renew Sustain Energy Rev* 82:2029–2038. <https://doi.org/10.1016/j.rser.2017.07.019>
- Chadee XT, Clarke RM (2014) Large-scale wind energy potential of the Caribbean region using near-surface reanalysis data. *Renew Sustain Energy Rev* 30:45–58. <https://doi.org/10.1016/j.rser.2013.09.018>
- Chadee X, Clarke RM (2018) Large-scale wind energy potential of the Caribbean region using near-surface reanalysis data. *Renew Sustain Energy Rev* 30:45–58. <https://doi.org/10.1016/j.rser.2013.09.018>

- Chadee XT, Seegobin NR, Ricardo C (2017) Optimizing the weather research and forecasting model for mapping the near-surface wind resources over the southernmost Caribbean Islands of Trinidad and Tobago. *Energies* 10(7):931. <https://doi.org/10.3390/en10070931>
- Chen AA, Stephens AJ, Koon R, Ashtine M, Koon KM (2020) Pathways to climate change mitigation and stable energy by 100% renewable for a small island: Jamaica as an example. *Renew Sustain Energy Rev* 121:109671. <https://doi.org/10.1016/j.rser.2019.109671>
- Christakos K, Varlas G, Chellotis I, Spyrou C, Aarnes AJ, Furevik BR (2020a) Characterization of wind-sea- and swell-induced wave energy along the Norwegian Coast. *Atmosphere* 11(2):166. <https://doi.org/10.3390/atmos11020166>
- Christakos K, Furevik BR, Aarnes OJ, Breivik Ø, Tuomi L, Byrkjedal Ø (2020b) The importance of wind forcing in fjord wave modelling. *Ocean Dyn* 70:57–75. <https://doi.org/10.1007/s10236-019-01323-w>
- Corrêa Radünz W, Sakagami Y, Haas R, Petry AP, Passos JC, Miqueletti M, Dias E (2020) The variability of wind resources in complex terrain and its relationship with atmospheric stability. *Energy Convers Manage* 222:113249. <https://doi.org/10.1016/j.enconman.2020.113249>
- Costoya X, deCastro M, Santos F, Sousa MC, Gómez-Gesteira M (2019) Projections of wind energy resources in the Caribbean for the 21st century. *Energy* 178:356–367. <https://doi.org/10.1016/j.energy.2019.04.121>
- de Farias EGG, Lorenzetti JA, Chapron B (2012) Swell and wind-sea distributions over the mid-latitude and tropical north Atlantic for the period 2002–2008. *Int J Oceanogr* 8:306723. <https://doi.org/10.1155/2012/306723>
- Dugstad A, Grimsrud KM, Kipperberg G, Lindhjem H, Navrud S (2020) Acceptance of wind power development and exposure – not-in-anybody’s-backyard. *Energy Policy* 147:111780. <https://doi.org/10.1016/j.enpol.2020.111780>
- Frank HP, Larsen SE, Højstrup J (2000) Simulated wind power offshore using different parameterizations for the sea surface roughness. *Wind Energy* 3(2):67–79
- Gao Q, Ertugrul N, Ding B, Negnevitsky M (2021). Offshore wind, wave and integrated energy conversion systems: a review and future. *Australasian Universities Power Engineering Conference, AUPEC 2020, Hobart, Australia*.
- Gideon RA, Bou-Zeid E (2021) Collocating offshore wind and wave generators to reduce power output variability: a multi-site analysis. *Renew Energy* 163:1548–1559. <https://doi.org/10.1016/j.renene.2020.09.047>
- Gkaraklova S, Chotzoglou P, Loukogeorgaki E (2020) Frequency-based performance analysis of an array of wave energy converters around a hybrid wind-wave monopile support structure. *J Mar Sci Eng* 9(1):2. <https://doi.org/10.3390/jmse9010002>
- Garcia C, Canals M (2015). Wave energy resource assessment and recoverable wave energy in Puerto Rico and the US Virgin Islands. *OCEANS*, 1–5. <https://doi.org/10.1109/OCEANS-Genova.2015.7271639>
- Glazman RE, Pilorz SH (1990) Effects of sea maturity on satellite altimeter measurements. *J Geophys Res Oceans* 95(C3):2857–2870. <https://doi.org/10.1029/JC095iC03p02857>
- Guillou N, Lavidas G, Ghalpalaïn G (2020) Wave energy resource assessment for exploitation - A review. *J Mar Sci Eng* 8(9):705. <https://doi.org/10.3390/jmse8090705>
- Hildebrandt A, Cossu R (2018) Misalignment and lag time of wind and wave occurrence based on 10 years measurements in the North Sea near the German Coast. *Coast Eng Proc* 1(36):13. <https://doi.org/10.9753/icce.v36.waves.13>
- Hildebrandt A, Schmidt B, Marx S (2019) Wind-wave misalignment and a combination method for direction dependent extreme incidents. *Ocean Eng* 180:10–22. <https://doi.org/10.1016/j.oceaneng.2019.03.034>
- Homayoun E, Ghassemi H, Ghafari H (2019) Power performance of the combined monopile wind turbine and floating buoy with heave-type wave energy converter. *Pol Marit Res* 26(3):107–114. <https://doi.org/10.2478/pomr-2019-0051>
- IRENA (2020). *Fostering a blue economy: offshore renewable energy*. International Renewable Energy Agency, Abu Dhabi.
- Jensen CU, Panduro TE, Lundhede T (2014) The vindication of Don Quixote: the impact of noise and visual pollution from wind turbines. *Land Econ* 90(4):668–682. <https://doi.org/10.3368/le.90.4.668>
- Jury MR (2018) Characteristics and meteorology of atlantic swells reaching the Caribbean. *J Coastal Res* 34:400–412. <https://doi.org/10.2112/JCOASTRES-D-17-00029.1>
- Kang T, Yang H (2019) Influence on floating offshore wind turbine structure by wave energy generated under extreme Metocean conditions. *J Korean Soc Manuf Technol Eng* 28(6):375–382. <https://doi.org/10.7735/ksmte.2019.28.6.375>
- Klöck C (2016) Fuelling the Pacific: aid for renewable energy across Pacific Island countries. *Renew Sustain Energy Rev* 58:311–318. <https://doi.org/10.1016/j.rser.2015.12.156>
- Koon RK, Marshall S, Morna D, McCallum R, Ashtine MI (2020) A review of Caribbean geothermal energy resource potential. *The West Indian Journal of Engineering* 42(2):37–43
- Kuang Y, Zhang Y, Zhou B, Li C, Cao Y, Li L (2016) A review of renewable energy utilization in islands. *Renew Sustain Energy Rev* 59:504–513. <https://doi.org/10.1016/j.rser.2016.01.014>
- Lee H, Yoo S, Huh S (2020) Public perspectives on reducing the environmental impact of onshore wind farms: a discrete choice experiment in South Korea. *Environ Sci Pollut Res* 27(20):25582–25599. <https://doi.org/10.1007/s11356-020-08949-0>
- Lemessy KG, Manohar K, Adeyanju A (2019). A review of wave energy conversion and its place in the Caribbean region. *The 13th European Wave and Tidal Energy Conference (EWTEC 2019), Napoli, Italy*.
- Liu Z, Chen H, Xu Y, Cheng Y, Zhao X (2021) Sensitivity analysis of wave direction in wave numerical model. *IOP Conf Ser Earth Environ Sci* 621:012076. <https://doi.org/10.1088/1755-1315/621/1/012076>
- Loukogeorgaki E, Vagiona DG, Vasileiou M (2018) Site selection of hybrid offshore wind and wave energy systems in Greece incorporating environmental impact assessment. *Energies* 11(8):2095. <https://doi.org/10.3390/en11082095>
- Ma X, Chen Y, Yi W, Wang Z (2021) Prediction of extreme wind speed for offshore wind farms considering parametrization of surface roughness. *Energies* 14(4):1033. <https://doi.org/10.3390/en14041033>
- Maria-Arenas A, Garrido AJ, Rusu E, Garrido I (2019) Control strategies applied to wave energy converters: state of the art. *Energies* 12(16):3115. <https://doi.org/10.3390/en12163115>
- Mazarakos T, Konispoliatis D, Katsaounis G, Polyzos S, Manolas D, Voutsinas S, Soukissian T, Mavrakos SA (2019). Numerical and experimental studies of a multi—purpose floating TLP structure for combined wind and wave energy exploitation. *Journal of Mediterranean Marine Science*, 20(4), 745–763. <https://doi.org/10.12681/mms.19366>
- Ochs A, Konold M, Auth K, Musolino E, Killeen P (2015). *Caribbean sustainable energy roadmap and strategy: baseline report and assessment*. Worldwatch Institute, Washington, DC. <https://doi.org/10.13140/RG.2.1.4351.1922>
- Optis M, Kumler A, Brodie J, Miles T (2021) Quantifying sensitivity in numerical weather prediction-modeled offshore wind speeds through an ensemble modeling approach. *Wind Energy* 24(9):957–973. <https://doi.org/10.1002/we.2611>

- Ortega S, Osorio AF, and Agudelo P (2013) Estimation of the wave power resource in the Caribbean Sea in areas with scarce instrumentation. Case Study: Isla Fuerte, Colombia. *Renew Energy* 57(C):240–248
- Ozkan C, Mayo T (2019) The renewable wave energy resource in coastal regions of the Florida peninsula. *Renewable Energy* 139:530–537. <https://doi.org/10.1016/j.renene.2019.02.090>
- Pérez-Collazo C, Pemberton R, Greaves D, Iglesias G (2019) Mono-pile-mounted wave energy converter for a hybrid wind-wave system. *Energy Convers Manag* 199:111971. <https://doi.org/10.1016/j.enconman.2019.111971>
- Porchetta S, Temel O, Muñoz-Esparza DS, Reuder J, Monbaliu J, van Beek J, van Lipzig N (2019) A new roughness length parameterization accounting for wind-wave (mis)alignment. *Atmospheric Chem Phys* 19:6681–6700. <https://doi.org/10.5194/acp-19-6681-2019>
- Praene JP, Fakra D, Benard F, Ayagapin L (2021) Comoros's energy review for promoting renewable energy sources. *Renew Energy* 169:885–893. <https://doi.org/10.1016/j.renene.2021.01.067>
- Pryor SC, Shepherd TJ, Bukovsky M, Barthelmie RJ (2020). Assessing the stability of wind resource and operating conditions. *Journal of Physics: Conference Series*, 1452 012084. NAWEA Wind Tech 2019, Amherst, MA, USA. <https://doi.org/10.1088/1742-6596/1452/1/012084>
- Ramos DA, Guedes V, Pereira RRS (2017). Atmospheric stability in wind resource assessment: development of a new tool for an accurate wind profile estimate. Brazil Wind Power 2016 Conference and Exhibition, Rio de Janeiro, Brazil.
- Reikard G, Robertson B, Bidlot J (2015) Combining wave energy with wind and solar: short-term forecasting. *Renew Energy* 81:442–456. <https://doi.org/10.1016/j.renene.2015.03.032>
- Rueda-Bayona JG, Guzmán A, Eras JJC, Silva-Casarin R, Bastidas-Arteaga E, Horrillo-Caraballo J (2019) Renewables energies in Colombia and the opportunity for the offshore wind technology. *J Clean Prod* 220:529–543. <https://doi.org/10.1016/j.jclepro.2019.02.174>
- Rusu E, Onea F (2019) An assessment of the wind and wave power potential in the island environment. *Energy* 175:830–846. <https://doi.org/10.1016/j.energy.2019.03.130>
- Rusu L, Raileanu AB, Onea F (2018) A comparative analysis of the wind and wave climate in the black sea along the shipping routes. *Water* 10(7):924. <https://doi.org/10.3390/w10070924>
- Semedo A, Sušelj K, Rutgersson A (2008). Variability of wind sea and swell waves in the North Atlantic based on ERA-40 Re-analysis. *Proceedings of the 8th European Wave and Tidal Energy Conference*, Uppsala, Sweden, 119–129.
- Semedo A, Sušelj K, Rutgersson A, Sterl A (2011) A global view on the wind sea and swell climate variability from ERA-40. *J Clim* 24(5):1461–1479. <https://doi.org/10.1175/2010JCLI3718.1>
- Shadman M, Estefen SE, Rodriguez CA, Nogueira ICM (2018) A geometrical optimization method applied to a heaving point absorber wave energy converter. *Renew Energy* 115:533–546. <https://doi.org/10.1016/j.renene.2017.08.055>
- Sterl S, Donk P, Willems P, Thiery W (2020) Turbines of the Caribbean: decarbonising Suriname's electricity mix through hydro-supported integration of wind power. *Renew Sustain Energy Rev* 134:110352. <https://doi.org/10.1016/j.rser.2020.110352>
- Silander MF, Moreno CGG (2019) On the spatial distribution of the wave energy resource in Puerto Rico and the United States Virgin Islands. *Renew Energy* 136:442–451. <https://doi.org/10.1016/j.renene.2018.12.120>
- Sørsum SH, Krokstad JR, Amdahl J (2019). Wind-wave directional effects on fatigue of bottom-fixed offshore wind turbine. *Journal of Physics: Conference Series*, 1356, 012011, 16th Deep Sea Off-shore Wind R&D Conference, Trondheim, Norway. <https://doi.org/10.1088/1742-6596/1356/1/012011>
- Verma AS, Jiang Z, Ren Z, Gao Z, Vedvik NP (2020) Effects of wind-wave misalignment on wind turbine blade mating process: impact velocities, blade root damages and structural safety assessment. *J Mar Sci Appl* 19(2):218–233. <https://doi.org/10.1007/s11804-020-00141-7>
- Wang Y, Zhang L, Michailides C, Wan L, Shi W (2020) Hydrodynamic response of a combined wind-wave marine energy structure. *J Mar Sci Eng* 8(4):253. <https://doi.org/10.3390/jmse8040253>
- Wang T, Yang Z, Wu W, Grear M (2018) A sensitivity analysis of the wind forcing effect on the accuracy of large-wave hindcasting. *J Mar Sci Eng* 6(4):139. <https://doi.org/10.3390/jmse6040139>
- Wei K, Shen Z, Ti Z, Qin S (2021) Trivariate joint probability model of typhoon-induced wind, wave and their time lag based on the numerical simulation of historical typhoons. *Stoch Env Res Risk Assess* 35:325–344. <https://doi.org/10.1007/s00477-020-01922-w>
- Wolsink M (2010) Near-shore wind power – protected seascapes, environmentalists' attitudes, and the technocratic planning perspective. *Land Use Policy* 27(2):195–203. <https://doi.org/10.1016/j.landusepol.2009.04.004>
- Zheng K, Sun J, Guan C, Shao W (2016) Analysis of the global swell and wind sea energy distribution using wave watch III. *Adv Meteorol* 2016(7):8419580. <https://doi.org/10.1155/2016/8419580>